An Investigation of the Polymorphism of a Potent Nonsteroidal Anti-inflammatory Drug Flunixin

Journal:	*CrystEngComm*
Manuscript ID	CE-ART-10-2019-001619.R1
Article Type:	Paper
Date Submitted by the Author:	09-Nov-2019
Complete List of Authors:	Liu, Hao; Wuhan Institute of Technology Yang, Xing; Wuhan Institute of Technology Wu, Shanyu; Nankai University Zhang, Mingtao; Purdue University System, IPPH; Nankai University, Parkin, Sean; University of Kentucky, Chemistry Cao, Shuang; Wuhan Institute of Technology Li, Tonglei; Purdue University, Yu, Faquan; Wuhan Institute of Technology Long, Sihui; Wuhan Institute of Technology, School of Chemical Engineering and Pharmacy

SCHOLARONE™
Manuscripts

An Investigation of the Polymorphism of a Potent

Nonsteroidal Anti-inflammatory Drug Flunixin

Hao Liu[1], Xing Yang[1], Shanyu Wu[2], Mingtao Zhang[2], Sean Parkin[3], Shuang Cao[1], Tonglei Li[4], Faquan Yu[1#], Sihui Long[1*]

1. *H. Liu, X. Yang, Dr. S. Cao, Dr. F. Yu, Dr. S. Long*

   Key Laboratory for Green Chemical Process of Ministry of Education

   Hubei Key Laboratory of Novel Reactor and Green Chemical Technology

   Hubei Engineering Research Center for Advanced Fine Chemicals

   School of Chemical Engineering and Pharmacy

   Wuhan Institute of Technology

   206 1st Rd Optics Valley, East Lake New Technology Development District, Wuhan, Hubei 430205,

   China

   Phone: (027) 87194980

   Email: fyuwucn@gmail.com

        Sihuilong@wit.edu.cn; longsihui@yahoo.com

2. *S. Wu, Dr. M. Zhang*

   Computational Center for Molecular Science,

   College of Chemistry,

   Nankai University, Tianjin, China

3. Dr. S. Parkin

   Department of Chemistry,

   University of Kentucky,

1

Lexington, Kentucky 40506, United States

4. Dr. T. Li

Department of Industrial and Physical Pharmacy,

Purdue University,

West Lafayette, Indiana 47907, United States

H. Liu and X. Yang contributed equally to this study.

Abstract:

Flunixin [2-(3-trifluoromethyl-2-methyl-phenylamino)-nicotinic acid, FLX], a potent nonsteroidal anti-inflammatory drug widely used in veterinary, was found to exist in at least two crystal forms (**I** and **II**), in contrast to clonixin [2-(3-chloro-2-methyl-phenylamino)-nicotinic acid, CLX], which exists in four solvent-free forms and multiple solvates. Form **I** was harvested from a variety of solvents and characterized by single-crystal X-ray diffraction, PXRD, FT-IR, and Raman spectroscopy. The crystal structure is sustained on the strong acid-pyridine hydrogen bond. Form **II** was generated by thermal treatment of form **I**. Other aspects of this polymorphic system were investigated both experimentally and theoretically. Quantum chemistry calculations were performed to shed light on the lack of polymorphs from solution-phase crystallization. Conformational scan of the dihedral angle C2-N7-C8-C9 (τ) revealed two stable conformations, one with the τ near 170°, and the other near 70°, corresponding to the molecule in the crystal. Hirshfeld analysis accounted for the major intermolecular interactions contributing to the overall stability of the crystal.

Keywords: flunixin, polymorphs, hydrogen bond, conformation, theoretical studies

Introduction

Nonsteroidal anti-inflammatory drugs (NSAIDs) are not only medicines for inflammation, but also analgesic, antipyretic ones, and they are widely used for the treatment of a variety of human and veterinary disease conditions involving pain and inflammation management.[1,2] NSAIDs are some of the more widely used therapeutic drugs. Classic NSAIDs include (but not limited to) salicylates, arylalkanoic acids, aryl- and heteroarylacetic acids, aryl- and heteroarylpropioic acids, N-arylanthranilic acids (also known as fenamic acids, FAs), and oxicams, *etc*.[3,4] These drugs exert their therapeutic effects by inhibiting prostaglandin (PG) synthesis through blocking access of arachidonic acid to its binding site on the cyclooxygenase enzyme.[5,6] N-Arylanthranilic acids are bio-isosteres of salicylic acid,[7] with mefenamic acid (MFA), flufenamic acid (FFA), clonixin (CLX), and flunixin (FLX) as representatives.[8] Among them, CLX and FLX are more closed related since they are both anilinonicotinic acids. Yet CLX is a human NSAID[9], and FLX is a potent veterinary one widely used in horses and other livestock, in the form of meglumine salt, for the treatment of inflammatory diseases or colics.[10,11] Currently the application of FLX in human diseases is also explored.[12] FAs are conformationally flexible diarylamines. Polymorphism, *i.e.*, the formation of more than one crystal form of a given molecule, is widely observed in FAs and other compounds as multiple forms have been found for them.[13,14] For example, for mefenamic acid two polymorphs (**I** and **II**) have been reported.[15] Nine polymorphs of FFA have been investigated,[16] and tolfenamic acid has been reported to have at least five forms.[17] In the past decade, our lab has been investigating the pharmaceutical potential and polymorphism of FAs, particularly CLX and its derivatives.[8,18]A series of CLX and FA analogues has been synthesized and their polymorphic behavior have been studied experimentally and theoretically.[19] Among them, several highly polymorphic compounds stand out. For example, four forms have been discovered for 2-(phenylamino)nicotinic acid [2-PNA] and 2-[methyl(phenyl)amino]nicotinic acid (2-MPNA), respectively.[20,21] Even for CLX, 30 years after the first report of polymorphism of it, we have found it tends to form solvates with DMF and DMF-like solvents.[8] In contrast, FLX was first

synthesized in 1974[22] and ever since has been widely used in the control of pain and inflammation as a veterinary medicine and recently its effect on the uterine mobility of equine embryos has been investigated.[23] Yet, its polymorphism has never been studied.

In this work, we attempted to shed light on the solid state properties of FLX, a compound closely resembles CLX structurally. As seen, the only difference between CLX and FLX is that Cl at the 3 position of CLX is replaced with CF_3 in FLX (Scheme 1), which is a strategy widely used in medicinal chemistry.[24] Intuitively, we would expect FLX to be polymorphic, just as does CLX. Yet, since CF_3 is not the same as Cl, difference in solid property could be expected. In reality, only one form was obtained from crystallization in all the solvents used. Thus, we also tried to investigate the polymorphic behavior of FLX theoretically.
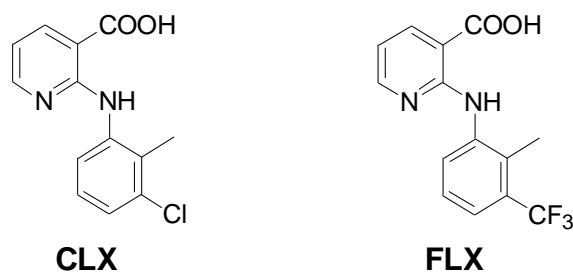
Scheme 1 Structure of CLX and FLX

2. Experimental Section

2.1. Materials

All chemicals were purchased from commercial sources: 2-methyl-3-trifluoromethyl-phenylamine was from Bide Pharmatech Ltd. (Shanghai, China); pyridine, 2-chloronicotinic acid and *p*-TsOH were from Aladdin Industrial Corporation; and solvents for crystal growth were from Sinopharm Chemical Reagent Co., Ltd (Shanghai, China), and were used as received.

2.2. Synthesis

FLX was synthesized by reacting 2-chloronicotinic acid with 2-methyl-3-trifluoromethyl-phenylamine

with *p*-TsOH as catalyst under a nucleophilic aromatic substitution (SNAr) mechanism according to a literature procedure and purified by recrystallization from MeOH (Scheme 2).[20]
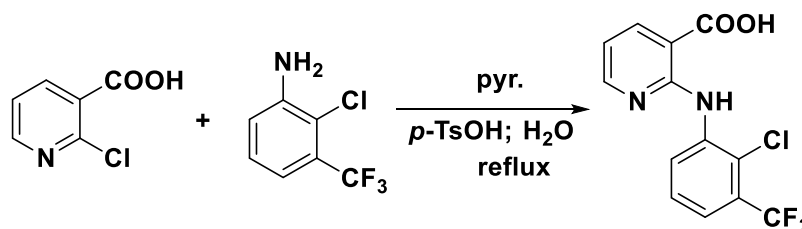
Scheme 2 Synthesis of FLX

2-Chloronictinic acid (2.0 g, 12.7 mmol) and 2-methyl-3-trifluoromethyl-phenylamine (1.8 g, 12.9 mmol) were suspended in pyridine (1.1 g, 13.7 mmol), *p*-TsOH (0.6 g, 3.2 mmol) in 10 mL of water was added to the mixture. The resulting system was refluxed overnight and then it was cooled to room temperature. The product precipitated and was recovered by filtration, and further purified by crystallization in MeOH (2.4 g, yield%: 73). The purity of the final product is over 99%.

^{1}H NMR (400 MHz, DMSO-*d₆*) δ ppm 10.30 (s, 1H), 8.34 (m, 1H), 8.27 (m, 1H), 8.11 (d, 1H), 7.19 (m, 2H), 6.87 (m, 1H), 2.33 (s, 3H); ^{13}C NMR (125 MHz, DMSO-*d₆*) δ ppm 169.7, 156.3, 153.1, 141.0, 140.3, 128.6, 127.7, 126.9, 126.2, 124.1, 120.6, 114.7, 108.4, 14.1; IR (KBr, cm^{-1}) 3239 (w), 2460 (w), 1677 (s), 1510 (s), 1242 (m), 1121 (s); EI-MS (MH$^+$) 297; mp 235 °C.

2.2. Crystallization

Since FLX and CLX are structurally similar, naturally we expected them to behave alike during crystallization. The same growth conditions used for CLX were applied to the crystal generation for FLX.[8] A detailed description of the procedure can be found in the Supporting Information (SI). The same form was produced by slow evaporation in all the solvents used. Slow cooling was also used for crystal growth (see SI for details). All crystallization experiments were conducted in an unmodified atmosphere. The identity of the crystals was confirmed by either single-crystal X-ray or powder X-ray diffraction. The crystallization results are listed in Table 1.

Table 1 Polymorph Screening of FLX

solvent	growth condition	form
ethyl acetate	slow evaporation	**I**
ethyl acetate	slow cooling	**I**
methanol	slow evaporation	**I**
methanol	slow cooling	**I**
ethanol	slow evaporation	**I**
ethanol	slow cooling	**I**
acetone	slow evaporation	**I**
acetone	slow cooling	**I**
acetonitrile	slow evaporation	**I**
iso-propanol	slow evaporation	**I**
water	slow evaporation	**I**
ether	slow evaporation	**I**
dichloromethane	slow evaporation	**I**
dimethylformamide	slow evaporation	**I**
acetic acid	slow evaporation	**I**
benzene	slow evaporation	**I**
dimethyl sulfoxide	slow cooling	**I**

2.3. Characterization

The crystal structure of FLX was determined by single-crystal X-ray diffraction (SCXRD). Powder X-ray diffraction (PXRD) was applied for bulk sample. The thermal behavior of FLX was investigated by differential scanning calorimetry (DSC). IR and Raman spectra were measured for FLX samples. The experimental details for each characterization were described in SI.

2.4. Computational Details

The Gavezzotti's UNI intermolecular potentials of all crystals were investigated first.[25,26] All the CLX dimers were extracted from the experimental crystal structures. FLX dimers were simulated by substituting the Cl in their corresponding CLX forms with CF_3 in order to compare and explain the difference between CLX and FLX. All dimers discussed here were optimized at the B3LYP/6-311G** level with dispersion corrections (GD3BJ) [27] by Gaussian16.[28] Single point energy calculations based on the optimized structures were performed with a larger basis set (6-311+G**). For both optimization and single point calculations, solvation was implicitly accounted for by the SMD[29] continuum solvation

model. Three typical solvents, water (H_2O), benzene, and dichloromethane (DCM) were selected based on their polarity difference. All calculations were performed at 1atm and 298.15K. Stabilization energy (ΔE) was defined as $\Delta E = E(dimer) - 2*E(monomer)$, in which E(monomer) refers to the energy of the optimized single molecule in the corresponding solvent, and E(dimer) refers to the energy of the optimized dimer. The sum of the stabilization energies of the assumed dimers was used to estimate and compare the thermodynamic stabilities of the possible corresponding crystal forms between CLX and FLX. The relaxed potential energy surface scan for the dihedral angle was conducted at B3LYP/6-311+G** with a step of 10 degrees. Hirshfeld surface analysis[30,31] was carried out and its fingerprint plot revealed intermolecular contacts within the crystal structure, providing insight into the intermolecular interactions. The relative contributions of various interactions by Hirshfeld surface were calculated with CrystalExplorer.[32]

3. Results and Discussion

3.1. Crystal Structures

In contrast to four solvent-free polymorphic forms and one solvate found for CLX, only one crystal form was obtained for FLX through crystallization in all the solvents used. No solvate was harvested from DMF. The crystal is monoclinic, space group $P2_1/c$ (Z = 4). Crystallographic data of form **I** (both LT and RT) and CLX-**I** are listed in Table 2; complete CIF files are provided in the Supporting Information. There is one formula unit in the asymmetric unit. These crystallographically independent molecules are conformationally similar to those in CLX−**I-LT** as suggested by the dihedral angle between the two aromatic rings in the molecules (68.22 (5)° for CLX-**I-LT**, 69.97(4)° for FLX (LT) and 71.14 (5) for FLX (RT), respectively) (Figure 3).
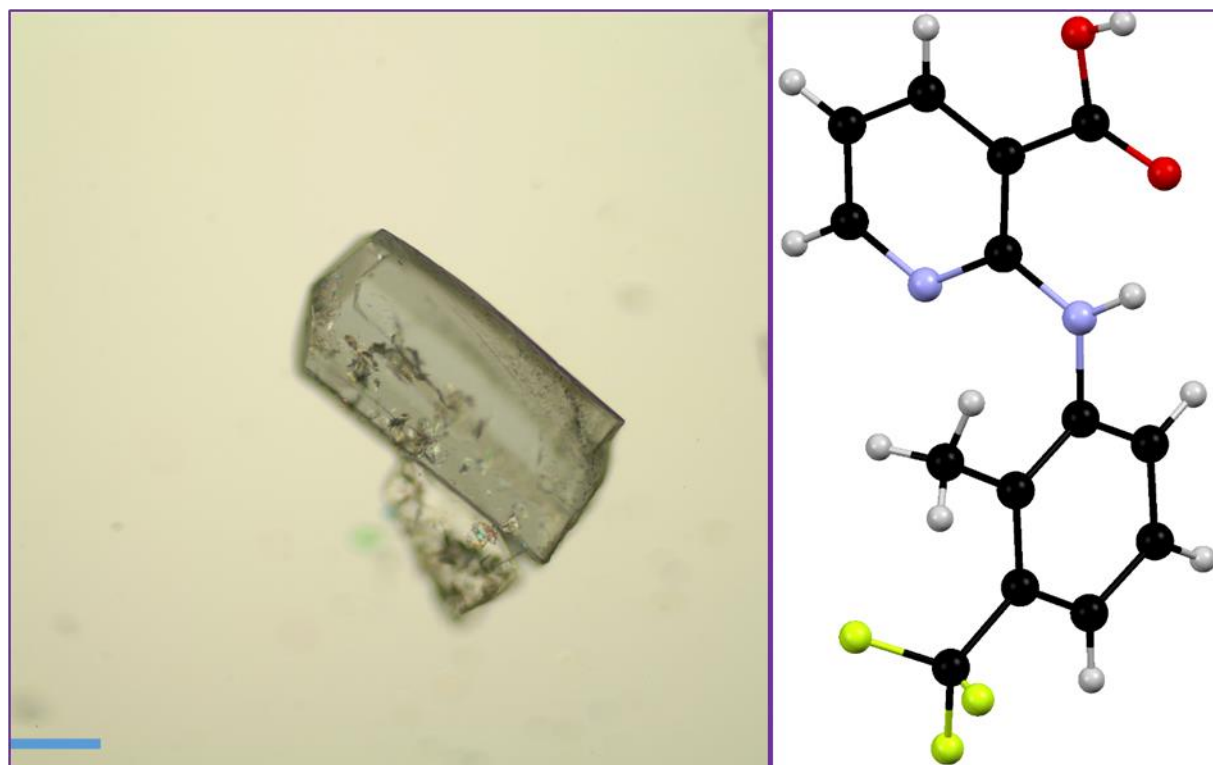
Figure 1. Crystals and conformer of FLX. Scale bar 0.2 mm.

Table 2 Crystallographic Data of Form **I** of CLX and FLX (both LT and RT)

	I (CLX)	FLX (LT)	FLX (RT)
formula	$C_{13}H_{11}ClN_2O_2$	$C_{14}H_{11}F_3N_2O_2$	$C_{14}H_{11}F_3N_2O_2$
formula weight	262.69	296.25	296.25
crystal size (mm)	0.20 x 0.20 x 0.12	0.50 x 0.35 x 0.30	0.50 x 0.35 x 0.30
crystal system	monoclinic	monoclinic	monoclinic
space group	$P2_1/c$	$P2_1/c$	$P2_1/c$
$a/Å$	7.479(1)	7.5380(1)	7.68546(13)
$b/Å$	14.162(2)	14.0607(2)	14.1282(2)
$c/Å$	11.582(2)	12.3766(1)	12.49862(17)
$a/°$	90.00	90.00	90.00
$\beta/°$	101.55(1)	103.3203(5)	102.1605(15)
$\gamma/°$	90.00	90.00	90.00
Z, Z'	4, 1	4, 1	4, 1
$V/Å^3$	1201.9(3)	1276.50(3)	1326.67(4)
$D_{cal}/g·cm^{-3}$	1.452	1.542	1.483
T/K	90.0 (2)	90.0 (2)	293(2)
abs coeff (mm^{-1})	0.312	0.134	1.120
F(000)	544	608	608
2θ range(deg)	2.30-27.50	2.23-25.98	4.4785-66.496
limiting indices	-9≤h≤9 -18≤k≤18 -15≤l≤15	-9≤h≤9 -16≤k≤16 -15≤l≤15	-7≤h≤8 -16≤k≤16 -14≤l≤14
completeness to 2θ	99.8%	98.2%	99.5%

Unique reflections	2264	2157	2037
$R_1[I>2\sigma(I)]$	4.66	0.0391	0.0393
wR_2 (all data)	0.121	0.0971	0.1074

The crystal structure of FLX is isostructural to that of CLX form **I** as can be seen from the crystallographic data. The molecule in the asymmetric unit is highly twisted as suggested by the dihedral angel of 69.97 (4)^{o} between the pyridine ring and the benzene ring, similar to that of 68.22 (5)^{o} in CLX-**I**. Due to the nonplanarity of the molecule, the crystals are colorless and the energetically more favorable hydrogen bond between the carboxylic acid and pyridine N is observed (C(6) in graph-set notation).[32,33] This is in agreement with the general rule established in our recent study regarding the formation of either the acid-acid homosynthon or the acid-pyridine heterosynthon in 2-PNA analogs, *i.e.*, if the dihedral angle between the pyridine ring and the benzene ring is over 30°, the acid-pyridine heterosynthon, otherwise the acid-acid homosynthon, will be formed.[34] The hydrogen bond parameters are 1.846 Å for bond length and 173.73^{o} for bond angle. Other than the intermolecular hydrogen bond, there is also an intramolecular hydrogen bond in each molecule between the NH that bridges the two aromatic rings and the carbonyl O of the carboxylic acid (S6), with a bond length of 1.961 Å and bond angle of 134.79^{o} (Figure 2).
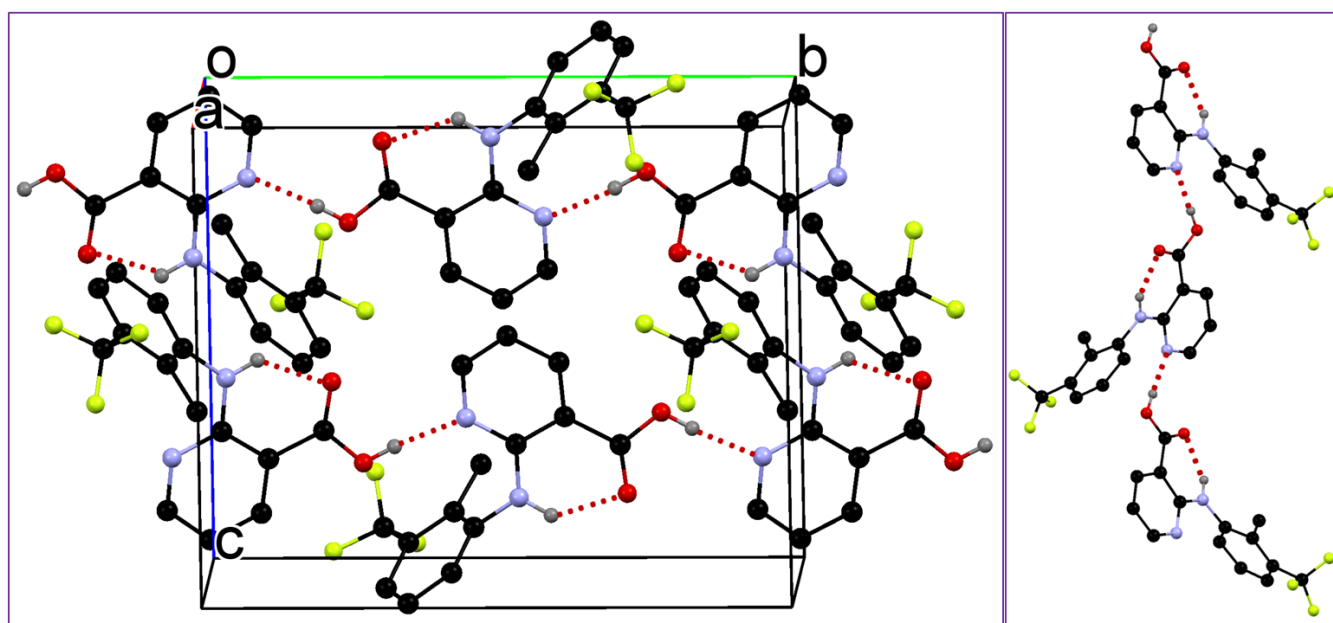
Figure 2. Crystal packing of FLX (for clarity, hydrogens not involved in hydrogen bonding are

omitted).
3.2. Thermal Properties

We resorted to DSC to investigate the thermal properties of FLX, and the DSC thermogram is shown in Figure 5. Upon heating, the crystals grown from different solvents showed two thermal events, the minor one with an onset temperature of 220 $^\circ$C which seemed to be a phase transition which led to a new form and the major one next to it with an onset temperature of 227 $^\circ$C, which was the melting of the new form. To confirm the formation of the new polymorph, the sample was cooled down to room temperature when it was heated right after the phase transition temperature, and when the new form was heated again, only one thermal event was observed (Figure 3).
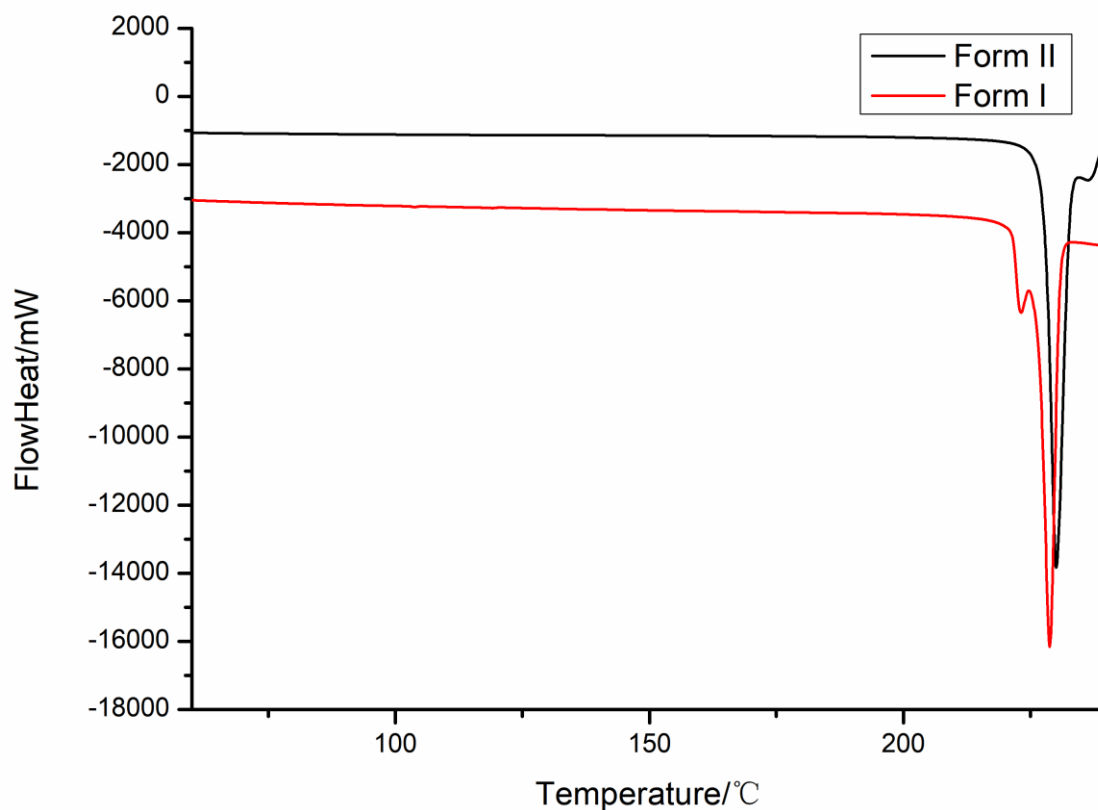
Figure 3. DSC thermograms of FLX
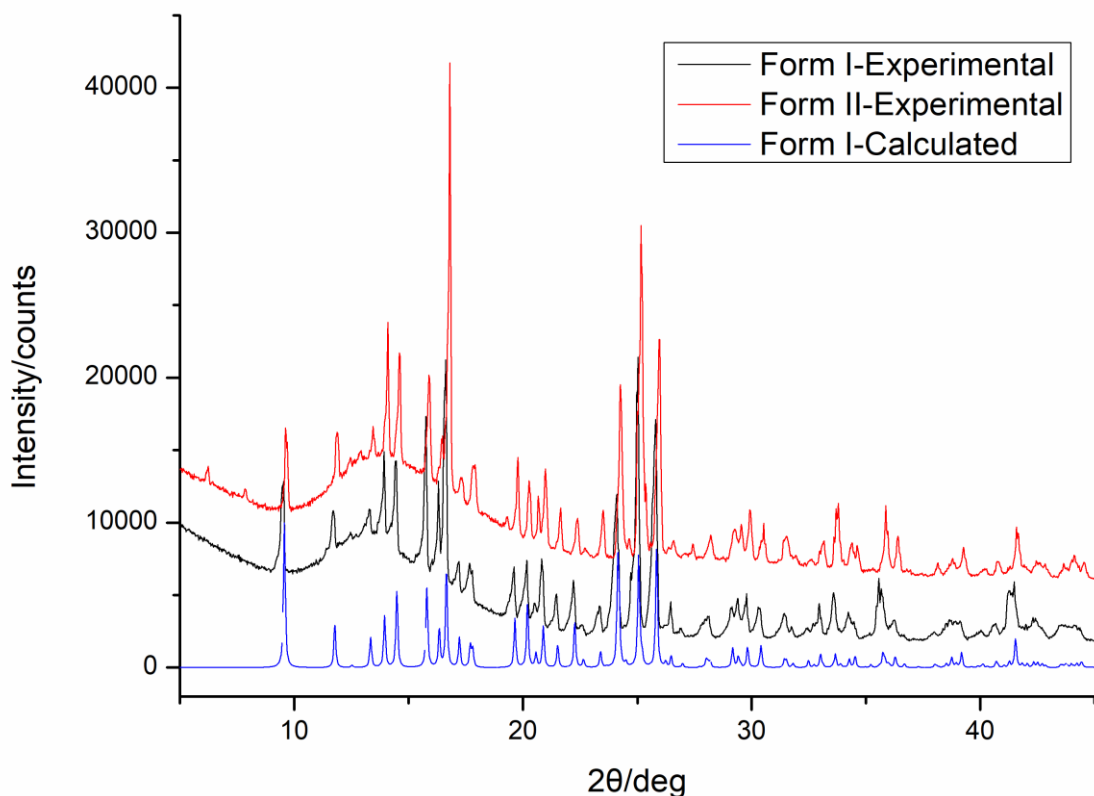
Figure 4. PXRD patterns of the two forms of FLX.

Figure 4 shows the powder X-ray diffraction patterns of crystals grown from solvents and obtained after thermal treatment of the original crystals, along with PXRD patterns calculated from the single-crystal structure determined at 293 K of form **I**.
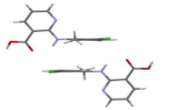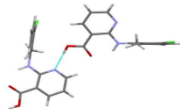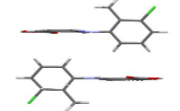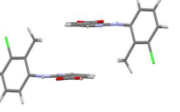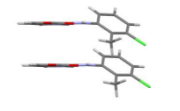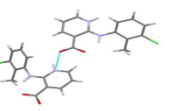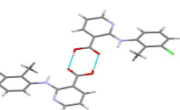
3.3. Computational Results

The only difference between CLX and FLX was that Cl at the 3 position of CLX was replaced with CF_3 in FLX. CLX is known to exist in four solvent-free and at least one solvate crystal forms, namely forms **I**, **II**, **III**, **IV**, and **S**. However, only one crystal form has been obtained from solution for FLX in this study. Theoretical calculations were made to compare and explain the polymorphism difference of CLX and FLX.

First, we tried to find out the dimers with strong interactions in all the known crystal forms according to

Gavezzotti's UNI intermolecular potentials. The results are listed in Tables 3 and 4. From the results we could conclude that the hydrogen bond dimers as well as π-π stacking dimers dominated the crystal structures..

Table 3 UNI intermolecular potentials in CLX crystals

crystal form	diagrammatic drawing	types of interactions	intermolecular potentials (kcal/mol)	number of contribution
I		π-π stacking between two benzenes	-11.6	1
		hydrogen bond between carboxylic acid and pyridine	-10.0	2
		H-π stacking between H and pyridine	-8.2	1
		π-π stacking between two pyridines	-6.5	1
II (zwitterions)		π-π stacking between two benzenes and two pyridines	-17.9	2
		hydrogen bond between carboxylate and pyridinium	-5.6	2
III		π-π stacking between two benzenes and two pyridines	-18.7	2
		hydrogen bond between two carboxylic acids	-9.5	1
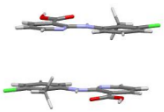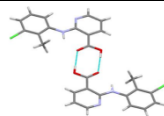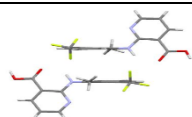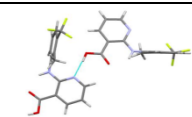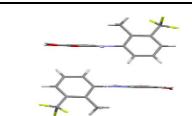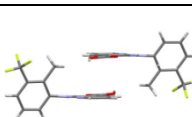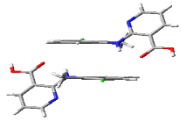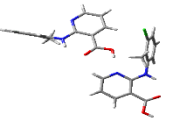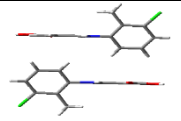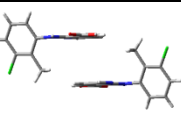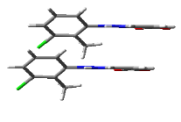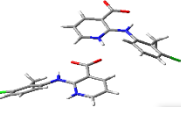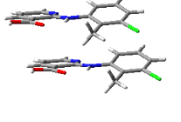
| IV | | antiparallel π-π stacking between benzene and pyridine | -18.8 | 2 |
| | | hydrogen bond between two carboxylic acids | -9.5 | 1 |

Table 4 UNI intermolecular potentials in FLX crystal

crystal form	diagrammatic drawing	types of interactions	intermolecular potentials (kcal/mol)	number of contribution
I		π-π stacking between two benzenes	-13	1
		hydrogen bond between carboxylic acid and pyridine	-10.3	2
		H-π stacking between H and pyridine	-7.2	1
		π-π stacking between two pyridines	-5.1	1

All dimers with their relative energies were listed in Tables 5 and 6. The total energies of the assumed crystals were then calculated based on the corresponding dimers and their contribution to different crystals. The summed up interaction energies were then compared in Table 7 to discuss the thermodynamic stability for the assumed crystals.

Table 5 Stabilization energies for CLX dimers in different solvents

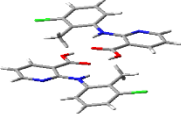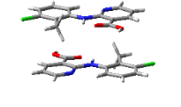| original structures extracted from crystal form	diagrammatic drawing	types of dimers	solvent		
			ΔE (kcal/mol) in H_2O	ΔE (kcal/mol) in Benzene	ΔE (kcal/mol) in DCM
I		π-π stacking between two benzenes	-14.34	-8.85	-9.37
		hydrogen bond between carboxylic acid and pyridine	-12.79	-13.33	-12.50
		H-π stacking between H and pyridine	-19.53	-8.58	-13.40
		π-π stacking between two pyridines	-13.77	-6.26	-7.35
II (zwitterions)		π-π stacking between two benzenes and two pyridines	-28.21	NA	-4.70
		hydrogen bond between carboxylate and pyridinium	-19.37	0.60	-10.49
III		π-π stacking between two benzenes and two pyridines	-20.47	-14.05	-14.49
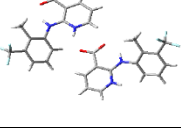
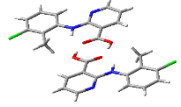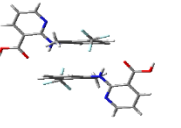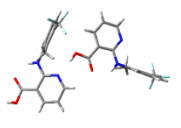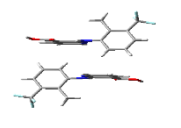|	diagrammatic drawing	types of dimers	ΔE (kcal/mol) in H₂O	ΔE (kcal/mol) in Benzene	ΔE (kcal/mol) in DCM
		hydrogen bond between carboxylic acid and pyridine	-11.86	-16.67	-13.90
IV		antiparallel π-π stacking between benzene and pyridine	-22.05	-17.22	-16.45
		hydrogen bond between two carboxylic acids	-11.65	-16.67	-13.79

Table 6 Stabilization energies for FLX dimers in different solvents

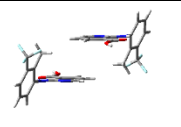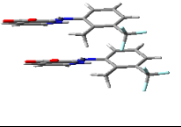| assumed dimers corresponding to CLX crystal form	diagrammatic drawing	types of dimers	solvent		
			ΔE (kcal/mol) in H_2O	ΔE (kcal/mol) in Benzene	ΔE (kcal/mol) in DCM
I		π-π stacking between two benzenes	-14.12	-8.43	-9.01
		hydrogen bond between carboxylic acid and pyridine	-12.10	-12.78	-12.09
		H-π stacking between H and pyridine	-18.72	-5.52	-6.22
		π-π stacking between two pyridines	-13.60	-5.98	-6.92
II (zwitterions)		π-π stacking between two benzenes and two pyridines	-23.38	-1.68	-9.56
		hydrogen bond between carboxylate and pyridinium	-18.00	0.00	-10.91

16
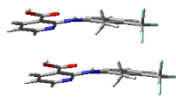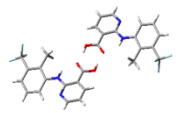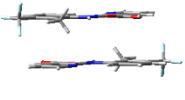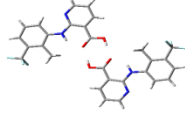
III		π-π stacking between two benzenes and two pyridines	-18.98	-13.65	-14.55
		hydrogen bond between two carboxylic acids	-11.39	-16.55	-13.80
IV		antiparallel π-π stacking between benzene and pyridine	-20.76	-15.83	-15.08
		hydrogen bond between two carboxylic acids	-11.55	-16.57	-13.81

Table 7 The sum of stabilization energies (ΔE) of assumed dimers of CLX and FLX in different solvents

corresponding crystal form	solvent	ΔE of CLX (kcal/mol)	ΔE of FLX (kcal/mol)
I	water	-73.22	-70.64
	benzene	-50.35	-45.50
	dichloromethane	-55.14	-46.33
II	water	-95.17	-82.75
	benzene	NA	-3.36
	dichloromethane	-30.38	-40.93
III	water	-52.80	-49.36
	benzene	-44.76	-43.84
	dichloromethane	-42.89	-42.90
IV	water	-55.74	-53.07
	benzene	-51.11	-48.22
	dichloromethane	-46.69	-43.96

The single molecule in CLX form **II** was a zwitterion, however. Zwitterions are not stable in non-polar

solvents, so form **II** was excluded in the non-polar solvent benzene. In addition, FLX dimer with acid-

pyridine hydrogen bond found in FLX form **I** would rotate along the hydrogen bond axis, so the restricted optimization was conducted for this dimer with the dihedral angle of the hydrogen bond plane fixed.

Our calculations reasonably explained why CLX and FLX mainly formed form **I** in water from the perspective of thermodynamics. According to the data, we could find that form **I** would be 20 Kcal/mol thermodynamically lower than forms **III** and **IV**.

Our calculations also explained why CLX and FLX could generate form **I** in dichloromethane. For CLX, a thermodynamic difference of -55.14 Kcal/mol could be obtained for the formation of form **I**, which was more stable than those of forming forms **III** and **IV**, which were -42.89 Kcal/mol, -46.69 Kcal/mol, respectively. As for FLX, the thermodynamic difference value of form **I** was -46.33 Kcal/mol, which was also more stable than those of forming forms **III** and **IV**, which were -42.90 Kcal/mol, -43.96 Kcal/mol, respectively. Therefore, the formation of form **I** could also be explained with its thermodynamic stability.

Our calculations reasonably explained the formation of form **IV** in benzene for CLX. The thermodynamic difference value was -51.11 Kcal/mol for form **IV** in benzene, while the values of forms **I** and **III** were -50.14 Kcal/mol and -44.76 Kcal/mol, respectively. Intriguingly, a similar trend was found for FLX calculations, which were not consistent with the experimental results. The limitation of calculations may be a possible explanation. A restricted optimization was adopted to avoid the rotation of the hydrogen bond axis when we optimized the acid-pyridine hydrogen bond dimers for FLX, which would give a higher energy for the unstable structure, while FLX molecules can form acid-pyridine hydrogen bond chains experimentally with the adjacent molecules hindering the rotation. Additionally, the growth of long chains will decrease the polarity of the molecules thus further decrease the repulsion from the nonpolar solvents. Therefore, the stability of form **I** was underestimated by the limitation of calculations. Thermodynamic difference for form **I** of FLX was calculated to be -45.5 Kcal/mol, which

was insufficient to compete with the thermodynamic difference of -48.22 Kcal/mol for form **IV**. Moreover, there are still many other factors affecting the crystallization including kinetic reasons which were not investigated here.

The relaxed potential energy surface (PES) evaluation was carried out *via* the flexible scanning of the dihedral angle C2-N7-C8-C9 (τ) of FLX based on its optimized structure. It can be found that there are two stable conformations (Figure 5). The near planar one with the τ near 170°, and the twisted one with τ near 70° (τ = 68.3° in the crystal). The energy difference is less than 2 kcal/mol, and the rotation energy barrier between them is only about 2.5 kcal/mol. It suggests the two conformations could be transformed freely with a dynamic equilibrium. Further optimizations of the two conformation were conducted, wherein the energy of the twisted conformation (τ = 70.7°) is slightly higher than that of the near planar one (τ = 172.4°) with only 1.36 kcal/mol including zero point energy (ZPE) correction, or 2.11kcal/mol in Gibbs free energy.
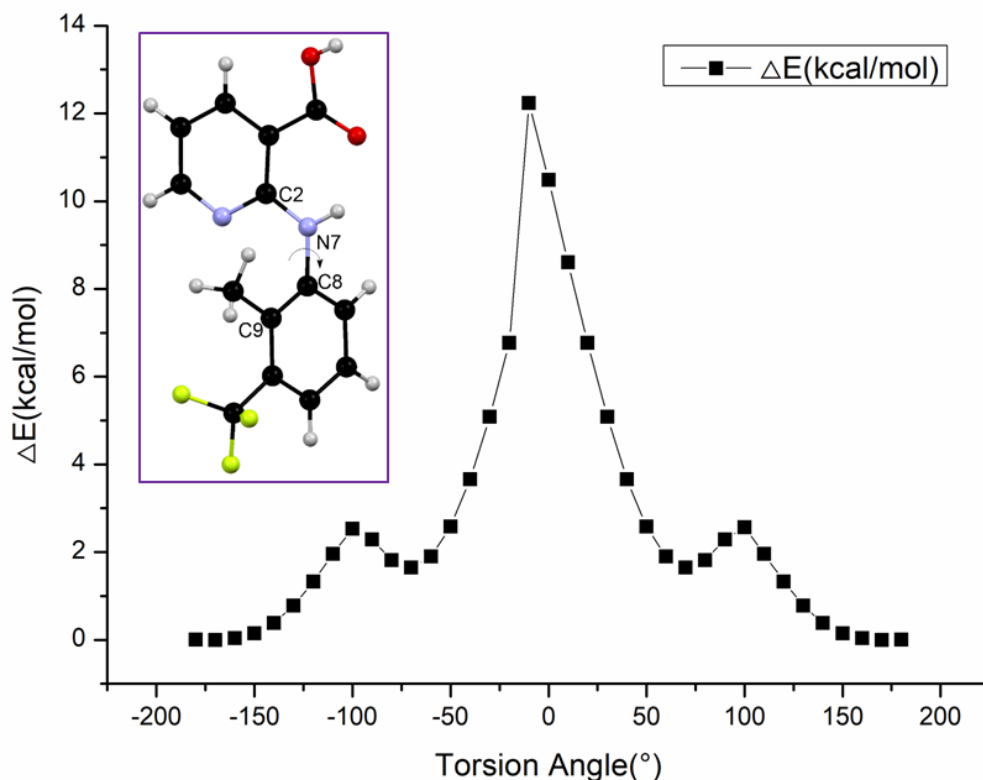
Figure 5. Relaxed potential energy surface (PES) scan along C2-N7-C8-C9

In Figure 6, it is evident that there are dominant interactions represented by the bright red, which is caused by hydrogen bond interaction between the N atom of pyridine and the H atom of the carboxyl acid. This dominant interaction is also represented by two spikes in the left-bottom region of the fingerprint plot (Figure 7). Other close contacts were also counted with their contributions to the Hirshfeld surface area in Figure 7. H-π interactions can be seen with C…H contacts with 18.1% of the Hirshfeld surface. H$\cdots$F contacts can also be found with a proportion of 22.7%. $\pi\cdots\pi$ stacking interactions were represented in C$\cdots$C contacts with a proportion of 2.9%. Hirshfeld surface analysis provided us a better understanding of the interactions of molecules in the crystal.
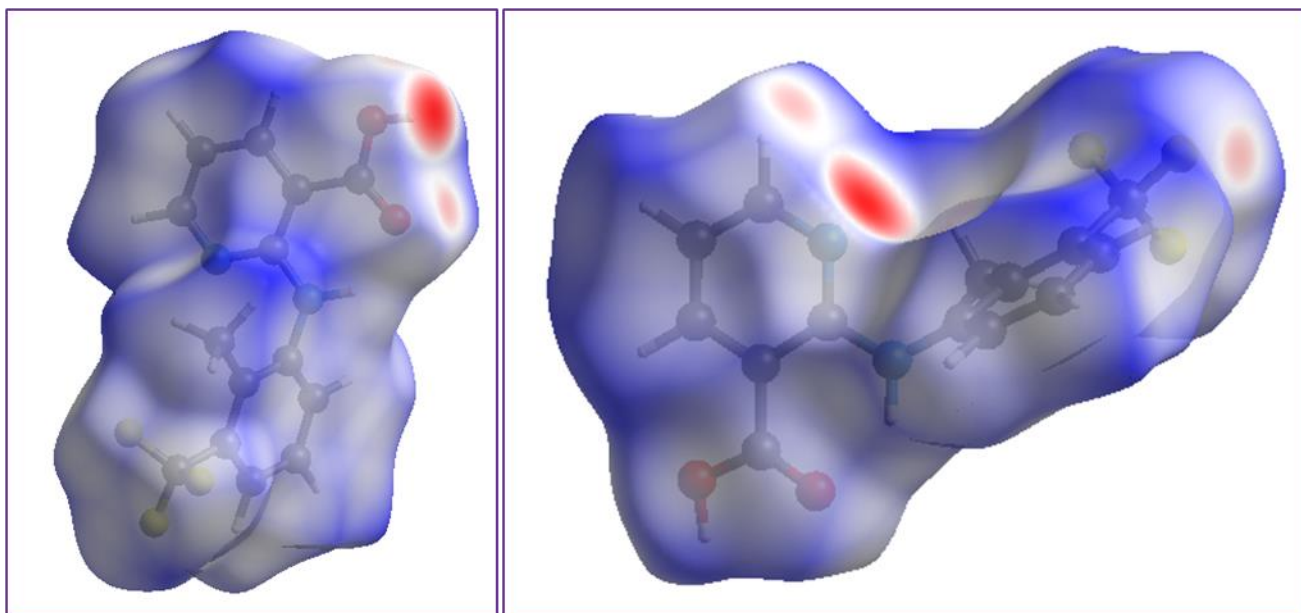
Figure 6. Hirshfeld surface with different orientations
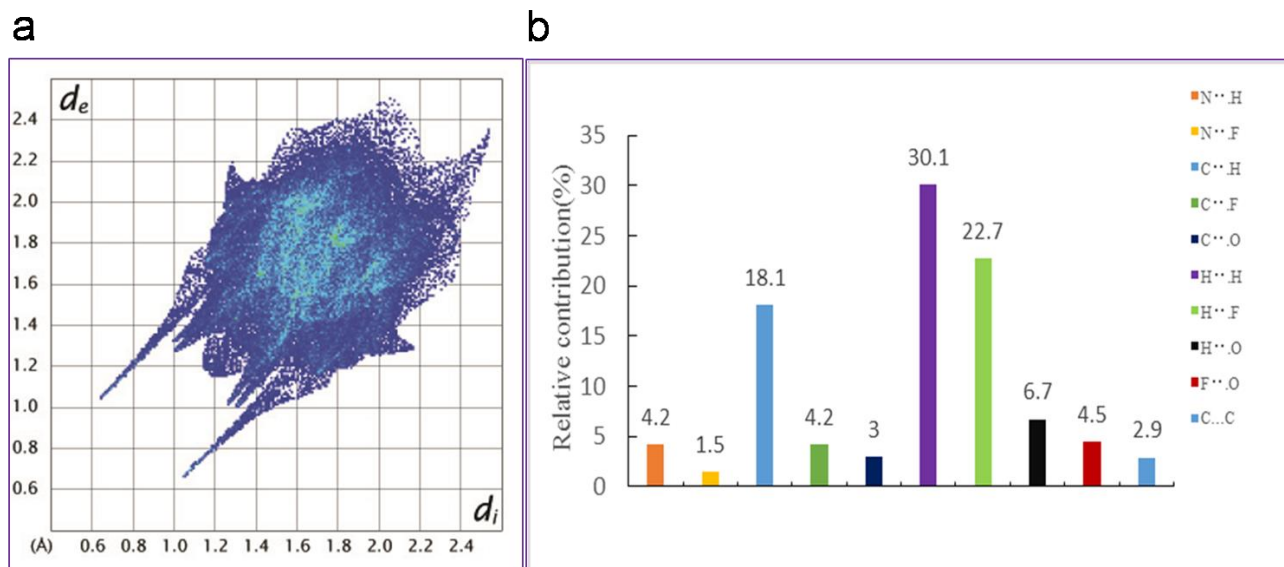
Figure 7. **a**. 2D fingerprint plots for FLX; **b**. relative contributions to the Hirshfeld surface by the various intermolecular contacts in the crystal.

4. Conclusions

FLX was synthesized through an S_NAr reaction and two crystal forms were obtained, one (**I**) through crystallization in solvents and the other (**II**) through thermal phase transition. Form **I** was fully characterized by SCXRD, PXRD, FT-IR and Raman. The crystal structure of form **I** is sustained on the acid-pyridine heterosynthon, same as that observed in form **I** of CLX. Form **I** transforms into form **II** upon thermal treatment. Theoretical calculations were performed to explain the lack of polymorphs in different solvents. Potential energy surface scan discloses two energetically close conformations, one with a torsion angle of 170° and the other 70°, which corresponds to the experimental conformation in the crystal. Hirshfeld analysis further delineates the contribution of individual interactions to the overall stability of each form. Considering the close resemblance between FLX and CLX, the "lack" of polymorphs of FLX deserves further investigation.

Supporting Information Available: Two crystal structures of FLX in the form of crystallographic information file (CIF) were deposited in the Cambridge Crystallographic Data Centre (CCDC) with accession codes 1957482 and 1957486. This material is available free of charge *via* the Internet at https://www.ccdc.cam.ac.uk/.

References:

1. S. Bajaj, S. S. Sambi and A. K. Madan, *Bioorg. Med. Chem.*, 2004, **12**, 3695.

2. P. Patrignani and C. Patrono, *Biochim. Biophys.*, 2015, **1851**, 422-432.

3. J. S. Kaltenbronn, R. A. Scherrer, F. W. Short, E. M. Jones, H. R. Beatty, M. M. Saka, C. V. Winder, J. Wax and W. R. Williamson, *Arzneim. Forsch.*, 1983, **33**, 621-627.

4. J. R. O'Brien, D. M. Oxon and F. C. Path, *Lancet*, 1968, **291**, 779-783.

5. G. A. Green, *Clin. Cornerstone.*, 2001, **3**, 50-59.

6. A. K. Dwivedi, V. Gurjar, S. Kumar and N. Singh, *Drug Discov Today.,* 2015, **20**, 863-873.

7. R. Hu, Y. Zhoujin, M. Liu, M. Zhang, S. Parkin, P. Zhou, J. Wang, F. Yu and S. Long, *RSC Adv.*, 2018, **8**, 15459-15470.

8. S. Long, T. Mao, P. Chen, M. Liu, S. Parkin, M. Zhang, T. Li, P. Zhou and F. Yu, *ChemistrySelect,* 2017, **2**, 4942-4950.

9. J. M. Lee, K. M. Park, S. J. Lim, M. K. Lee and C. K. Kim, *J. Pharm. Pharmacol.* 2002, **54**, 43-49.

10. J. E. Tomlinson, B. O. Wilder, K. M. Young and A. T. Blikslager, *Am. J. Vet. Res.*, 2004, **65**, 761-769.

11. S. Zamir, A. Rozov and E. Gootwine, *Veterinary Record.*, 2009, **165**, 265-266.

12. I. Reinholds, I. Pugajeva, D. Zacs, E. Lundanes, J. Rusko, I. Perkons and V. Bartkevics, *Environ. Monit. Assess.*, 2017, **189**, 568.

13. A. Kons, A. Berzin, A. Actiņs, T. Rekis, S. Smaalen and A. Mishnev, *Cryst. Growth Des.*, 2019, **19**, 4765-4773.

14. B. Hachuła, M. Zubko, P. Zajdel, M. Książek, J. Kusz, O. Starczewska, J. Janeka and W. Pisarski, *CrystEngComm.*, 2018, **20**, 1739-1745.

15. F. Kato, M. Otsuka and Y. Matsuda, *Int. J. Pharm.*, 2006, **321**,18-26.

16. V. L´opezmej´ıas, J. W. Kampf and A. J. Matzger, *J. Am. Chem. Soc.*, 2012, **134**, 9872-9875.

17. W. Tang, H. Mo, M. Zhang, S. Parkin, J. Gong, J. Wang, and T. Li, *J. Phys. Chem. B*, 2017, **121**,

10118-10124.

18. M. Liu, G. Shen, Z. Yuan, S. Parkin, F. Yu, M. Zhang, S. Long and T. Li, *Cryst. Growth Des.*, 2018, **18**, 7006-7014.

19. Y. Liu, M. Zhang, D. Xu, S. Parkin, T. Li, C. Li, Z. Yang, F. Yu and S Long, *Cryst. Growth Des.*, 2019, **19**, 3694-3703.

20. S. Long, S. Parkin, M. A. Siegler, A. Cammers and T. Li, *Cryst. Growth Des.*, 2008*, **8***, 4006-4013.

21. S. Long, S. Parkin, M. Siegler, C. P. Brock, A. Cammers and T. Li, *Cryst. Growth Des.*, 2008, **8**, 3137-3140.

22. M. H. Sherlock, U.S. Patent 3, 839, 344, **1974**.

23. C. T. C. Okada, V. P. Andrade, C. P. F. Dell'Aqua, M. Nichi, C. B. Fernandes, F. O. Papa and M. A. Alvarenga, *Theriogenology*, 2019, **123**, 132-138.

24. Y. Sasaki, M. Hirabuki, A. Ambo, H. Ouch and Y. Yamamoto, *Bioorg. Med. Chem. Lett.*, 2001, **11**, 327-329.

25. A. Gavezzotti, *Acc. Chem. Res.*,1994, **27**, 309-314.

26. A. Gavezzotti and G. Filippini, *J. Phys. Chem.*, 1994, **98** (18), 4831-4837.

27. S. Grimme, S. Ehrlich and L. Goerigk, *J. Comp. Chem.*, 2011, **32**, 1456-65.

28. M. J. Frisch, G. W. Trucks, H. B. Schlegel, G. E. Scuseria, M. A. Robb, J. R. Cheeseman, G. Scalmani, V. Barone, G. A. Petersson, H. Nakatsuji, X. Li, M. Caricato, A. V. Marenich, J. Bloino, B. G. Janesko, R. Gomperts, B. Mennucci, H. P. Hratchian, J. V. Ortiz, A. F. Izmaylov, J. L. Sonnenberg, D. Williams-Young, F. Ding, F. Lipparini, F. Egidi, J. Goings, B. Peng, A. Petrone, T. Henderson, D. Ranasinghe, V. G. Zakrzewski, J. Gao, N. Rega, G. Zheng, W. Liang, M. Hada, M. Ehara, K. Toyota, R. Fukuda, J. Hasegawa, M. Ishida, T. Nakajima, Y. Honda, O. Kitao, H. Nakai, T. Vreven, K. Throssell, J. A. Montgomery Jr, J. E. Peralta, F. Ogliaro, M. J. Bearpark, J. J. Heyd, E. N. Brothers, K. N. Kudin, V. N. Staroverov, T. A. Keith, R. Kobayashi, J. Normand, K. Raghavachari, A. P. Rendell, J. C. Burant, S. S. Iyengar, J. Tomasi, M. Cossi, J. M. Millam, M. Klene, C. Adamo, R. Cammi, J. W. Ochterski, R. L. Martin, K. Morokuma, O. Farkas, J. B. Foresman, D. J. Fox, Gaussian, *Inc., Wallingford CT*, 2016.

29. A. V. Marenich, C. J. Cramer and D. G. Truhlar, *J. Phys. Chem.*, 2009, **113**, 6378-96.

30. F. L. Hirshfeld, *Theor. Chim. Acta.*, 1977, **44**, 129-138.

31. M. A. Spackman and D. Jayatilaka, *CrystEngComm.*, 2009, **11**, 19-32.

32. S. K. Wolff, D. J. Grimwood, J. J. McKinnon, M. J. Turner, D. Jayatilaka and M. A. Spackman, University of Western Australia, 2012**.**

33. M. C. Etter, *Acc. Chem. Res.*, 1990, **23**, 120-126.

34. J. Bernstein and R. E. Davis, *Angew. Chem., Int. Ed.*, 1995, **34**, 1555-1573.

24